

Catch–Release System for Dosing and Recycling Silver(I) Catalyst with Status of Catalytic Activity Reported by Fluorescence

Indrajit Paul,[†] Nikita Mittal,[†] Soumen De,[†] Michael Bolte,[‡] and Michael Schmittl*^{†,‡}

[†]Center of Micro and Nanochemistry and Engineering, Organische Chemie I, Universität Siegen, Adolf-Reichwein Straße 2, D-57068 Siegen, Germany

[‡]Institut für Anorganische und Analytische Chemie, Goethe-Universität Frankfurt, Max-von-Laue-Straße 7, D-60438 Frankfurt (Main), Germany

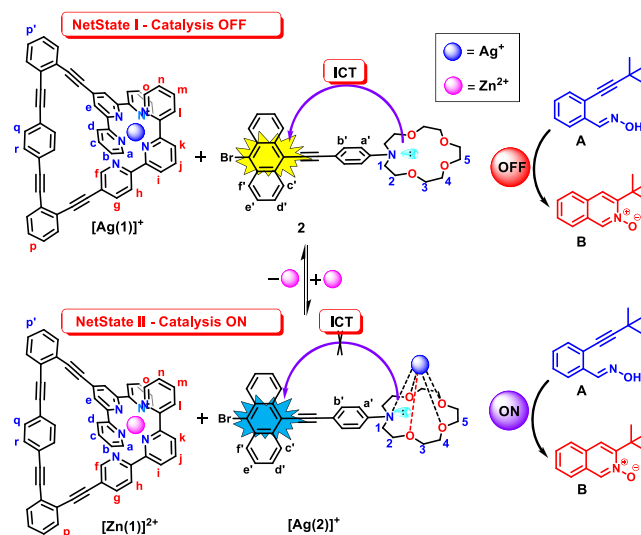
S Supporting Information

ABSTRACT: The silver(I) catch–release system composed of nanoswitch **1** and the anthracene-appended crown ether **2** is infallibly driven by chemical triggers and ion transfer. Any state of the silver(I) translocation is self-reported by a ratiometric emission signature at 472 and 554 nm. In the self-sorted networked state I, the silver(I) ions are tightly shielded inside nanoswitch [Ag(1)]⁺ (“catch”) so that their catalytic activity is zero while emission at 554 nm is maximum. Addition of zinc(II) releases silver(I) from [Ag(1)]⁺ and generates the catalytically active and fluorescent complex [Ag(2)]⁺. In this networked state II (“release”) both catalytic activity and emission at 472 nm are maximum. Removal of the original trigger regenerates networked state I. ON/OFF control and recycling of catalyst was demonstrated over three *in situ* cycles.

While metal-ion catalysis (Pd²⁺, Pt^{II}, Cu⁺, etc.)¹ is widespread, exact stoichiometry of redox- and light-sensitive ions, e.g. Ag⁺,² is often difficult to command. In particular, silver(I) is well-known for its photosensitivity³ so that controlling, recycling and reproducing its catalytic activity³ is often hampered.⁴ Herein, we describe the dependable generation of an anthracene-crown ether silver(I) complex with a built-in fluorescence-reporter system. While this complex is as catalytically active as free silver(I), it is noticeably more resistant to decomposition. Its multiuse utility is demonstrated in a chemically toggled catch–release system that allows continuous fine-tuning and monitoring of silver(I)-catalytic activity from OFF to ON. The chemically triggered *modus operandi* runs contrary to other catch–release systems,^{5,6} most of which are based on magnetic nanoparticles.⁷ The present work thus opens the arena of intermolecular communication,⁸ so far mostly studied for proof of concept,⁹ for practical purposes.

Design of the catch–release system (Scheme 1) has been inspired by recent progress in chemically networked nanoswitches¹⁰ and nanorotors¹¹ that enable ON/OFF-adjustment of copper(I) catalysis by an external trigger. Analogous regulation of sensitive silver(I) though is much more challenging and requires stabilization of silver(I) without loss of catalytic activity.⁴ In the present work both luminescence (ratiometric) and catalytic activity (ON/OFF) are com-

Scheme 1. Catch–Release of Catalytic Silver(I) Triggered by Zinc(II)



manded by the translocation of silver(I) from nanoswitch **1** to receptor **2**. In the initial networked state (NetState-I), silver(I) ions are tightly captured within the cavity of the triangular nanoswitch **1** (“catch”) so that catalysis is OFF. In this state the luminophore **2** is left uncoordinated exhibiting fluorescence at 554 nm. Upon addition of zinc(II) as trigger, nanoswitch [Ag(1)]⁺ will transmit silver(I) ions to the anthracene-crown ether **2** resulting in [Zn(1)]²⁺ and [Ag(2)]⁺. In NetState-II (“release”) fluorescence emerges at 472 nm and catalysis is ON.

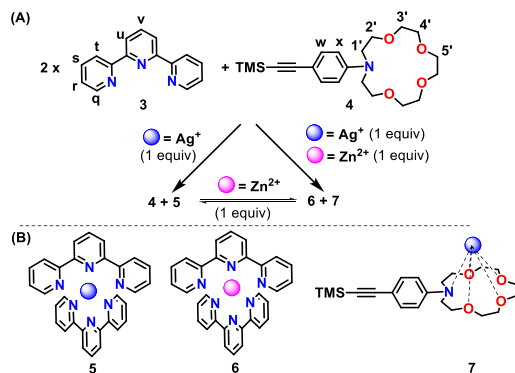
The details of this switchable ensemble were conceived along the following considerations. (1) Because of its two terpyridine binding sites, nanoswitch **1** should inhibit catalytic activity of silver(I), but should preferentially bind zinc(II) thus liberating Ag⁺ ions. (2) The azacrown-ether appended anthracene **2** should act as luminescence-responsive host for liberated silver(I). (3) The initial self-sorting¹² should place silver(I) preferentially in nanoswitch **1** over probe **2**. (4) Silver(I) should be stabilized by binding to the crown-ether site of **2** but still unfold catalytic activity. (5) Reactant and

Received: January 31, 2019

product of the catalytic process should not intervene with the catch–release protocol.

To design the exact binding sites in **1** and **2**, we tested the metal-ion dependent self-sorting by mixing of 2,2':6',2''-terpyridine (**3**), azacrown **4** and AgBF_4 in a ratio of 2:1:1 (Scheme 2). The homoleptic silver complex $5=[\text{Ag}(\mathbf{3})_2]^+$

Scheme 2. (A) Switching between Complexes 5, 6 and 7; (B) Structures of 5–7



formed selectively whereas azacrown-ether **4** remained free. This self-sorting is fully understandable on thermodynamic grounds, since **5** has a higher binding affinity ($\Delta\log K = 3.18$, Figures S46 and S47) toward silver(I) than **4**. Afterward, addition of 1.0 equiv of $\text{Zn}(\text{OTf})_2$ selectively translocated the silver ions from $5=[\text{Ag}(\mathbf{3})_2]^+$ to the azacrown receptor affording $7=[\text{Ag}(\mathbf{4})]^+$ and the zinc complex $6=[\text{Zn}(\mathbf{3})_2]^{2+}$.

Using this insight, nanoswitch **1** was conceived as a triangular scaffold with two terpyridine units. Complex $[\text{Ag}(\mathbf{1})]^+$ was prepared by mixing AgBF_4 (as standard solution in d_3 -acetonitrile) and nanoswitch **1** in d_2 -dichloromethane (1:50 v/v) at 25 °C and fully characterized by ^1H NMR, $^1\text{H}-^1\text{H}$ -COSY, UV–vis, ESI-MS and elemental analysis. For instance, a single peak at $m/z = 895.8$ (100%) in the electrospray-ionization mass spectrum (ESI-MS) attests formation of $[\text{Ag}(\mathbf{1})]^+$ (Figure S44). Analogously, complex $[\text{Zn}(\mathbf{1})]^{2+}$ was prepared from $\text{Zn}(\text{OTf})_2$ and nanoswitch **1** (1:1) (Figure S44).

Luminophore **2**, conceived as an anthracene with an appended N,O-crown-ether receptor, was synthesized (Scheme S1) and characterized (for X-ray, Figure 1A). The ethynyl

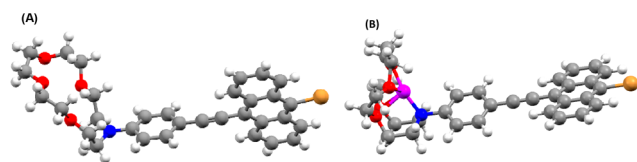


Figure 1. (A) X-ray crystal structure of **2**. Hydrogen atoms are shown in white; C, light gray; N, blue; O, red; Br, orange. (B) Ball and stick representation of the energy-minimized structure (B3LYP/3-21G) of $[\text{Ag}(\mathbf{2})]^+$.

linkage between fluorophore and binding site was expected to entail an intense intramolecular charge transfer (ICT) from the nitrogen to the anthracene. Anthracene was chosen as a reporter element due to its known excitation/emission profile with high fluorescence quantum efficiency.

In $\text{CH}_2\text{Cl}_2:\text{CH}_3\text{CN}$ (50:1), luminophore **2** exhibits absorptions at $\lambda = 255, 411,$ and 435 nm (broad). In a UV–vis titration with silver tetrafluoroborate, one observes the appearance of a new lower-energy band centered around 268 nm that increases upon progressive addition of the metal ion at the expense of the band at $\lambda = 255$ nm. These findings strongly indicate that silver(I) ion binds at the aza-15-crown-5 site. Upon exceeding one equiv of silver(I), the absorbance at $\lambda = 268$ nm remained almost constant, suggesting formation of a 1:1 complex. This stoichiometry was corroborated by a Job plot analysis and a peak at $m/z = 682.2$ in the ESI-MS (for the computed structure, see Figure 1B). Binding of silver(I) ions toward receptor **2** was determined as $\log K = 3.66 \pm 0.29$ (Figure S47).

Figure 2A (inset) illustrates the emission of reporter **2** when excited at $\lambda = 410$ nm. In the absence of silver(I), **2** exhibits a

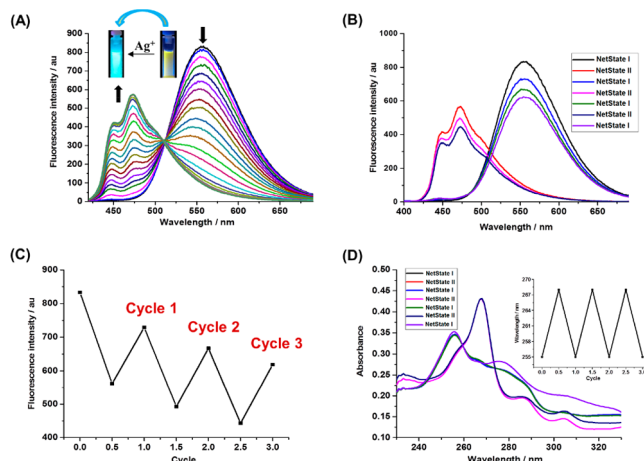


Figure 2. (A) Ratiometric fluorescence titration of **2** ($2.78 \mu\text{M}$) with silver(I) in $\text{CH}_2\text{Cl}_2:\text{CH}_3\text{CN} = 50:1$. (B) Reversibility of chemical network over three cycles monitored by fluorescence intensity at $\lambda = 554$ and 472 nm. (C) Multiple cycles monitored at $\lambda = 554$ nm. (D) Reversible chemical communication monitored by UV–vis.

strong emission at $\lambda = 554$ nm with a bright yellow fluorescence, characteristic of conjugated anthracene derivatives. As expected by design, in a titration of **2** with silver(I), the initial peak at $\lambda = 554$ nm gradually decreases while simultaneously emissions at $\lambda = 448$ and 472 nm emerge. The sky-blue emission was assigned to complex $[\text{Ag}(\mathbf{2})]^+$. The large blue shift is attributed to a silver(I)-induced restriction of the intramolecular charge transfer process (ICT). The fluorescence quantum yield of **2** ($\Phi = 0.58$) was decreased to $\Phi = 0.28$ upon addition of one equiv of $\text{Ag}(\text{I})$ ions.

For testing the required self-sorting, we blended nanoswitch **1**, reporter **2** and AgBF_4 in a 1:1:1 ratio in d_2 -dichloromethane. The resultant NetState-I, i.e. $[\text{Ag}(\mathbf{1})]^+ + \mathbf{2}$, was ascertained in the ESI-MS by $m/z = 895.8$ (100%) with an isotopic distribution matching exactly the theoretical one of $[\text{Ag}(\mathbf{1})]^+$. Moreover, in the ^1H NMR (Figure 3) protons a-H, b-H, and c-H are diagnostically shifted from 8.68, 7.25, and 7.75 ppm to 8.08, 7.20, and 7.70 ppm alike in isolated $[\text{Ag}(\mathbf{1})]^+$. Proton signals for a'-H and b'-H at 6.55 and 7.61 ppm correspond to free **2**. In addition, the UV–vis spectrum shows bands at $\lambda = 255, 411,$ and 435 nm that are diagnostic of free **2** and a new absorption at $\lambda = 321$ nm corresponding to $[\text{Ag}(\mathbf{1})]^+$.

Upon addition of 1.0 equiv of $\text{Zn}(\text{OTf})_2$ (as a standard solution in CD_3CN) to NetState-I = $[\text{Ag}(\mathbf{1})]^+ + \mathbf{2}$, a second

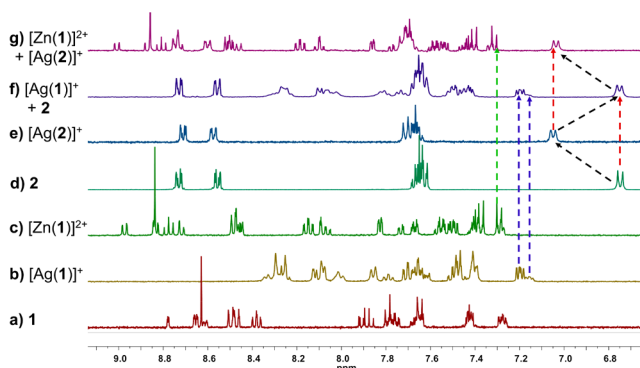


Figure 3. Comparison of partial ^1H NMR spectra (400 MHz, CD_2Cl_2 , 298 K) of (a) switch **1**, (b) $[\text{Ag}(\text{I})]^+$, (c) $[\text{Zn}(\text{I})]^{2+}$, (d) luminophore **2**, (e) $[\text{Ag}(\text{II})]^+$, (f) $[\text{Ag}(\text{I})]^+ + \mathbf{2}$, and (g) $[\text{Zn}(\text{I})]^{2+} + [\text{Ag}(\text{II})]^+$.

quantitative self-sorting generated NetState-II = $[\text{Zn}(\text{I})]^{2+} + [\text{Ag}(\text{II})]^+$. In the ESI-MS a singly charged species at $m/z = 1001.4$ (95%) and a doubly charged one at $m/z = 427.7$ (15%) attest presence of $[\text{Zn}(\text{I})]^{2+}$ (Figure S44). Moreover, a singly charged species at $m/z = 682.2$ (100%) represents $[\text{Ag}(\text{II})]^+$. Diagnostically, in the ^1H NMR, protons a-H, b-H, and c-H are shifted to 8.50, 8.15, and 7.50 ppm matching exactly the data of $[\text{Zn}(\text{I})]^{2+}$ while $[\text{Ag}(\text{II})]^+$ is equally recognized by its diagnostic shifts.

Kinetics of Ag^+ release and translocation, i.e. of the zinc(II)-induced self-sorting, was determined using UV-vis spectroscopy at 25 °C. Upon addition of 1.0 equiv of $\text{Zn}(\text{OTf})_2$ to NetState-I, the band at $\lambda = 321$ nm corresponding to $[\text{Ag}(\text{I})]^+$ shifted within 1.5 min to 345 nm, an absorption representing $[\text{Zn}(\text{I})]^{2+}$. Synchronously the absorption of **2** at $\lambda = 460$ nm experienced a blue shift to 410 nm. Interestingly, in absence of **2** the replacement of silver(I) by zinc(II) in **1** was a bit slower taking almost 2 min for completion. Full reversal back to NetState-I was accomplished within 2.5 min by addition of hexacyclen as scavenger for zinc(II).

Multiple NetState-I \leftrightarrow NetState-II interconversions were established from the ^1H NMR (Figure 4) and fluorescence spectra. Upon addition of $\text{Zn}(\text{OTf})_2$ to NetState I the fluorescence changes from yellow ($\lambda = 554$ nm) to sky-blue ($\lambda = 448$ and 472 nm) due to the formation of $[\text{Ag}(\text{II})]^+$. The ratiometric emission profile was reproduced over three cycles (Figure 2B,C) with a small decline in emission intensity.

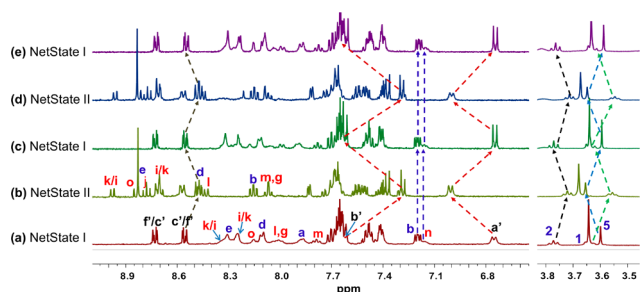
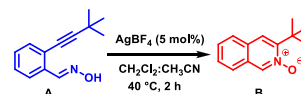


Figure 4. Partial spectra (400 MHz, CD_2Cl_2 , 298 K) showing the reliable switching between NetState I and II over 2.5 cycles. (a) After mixing of AgBF_4 , **1**, and **2** in 1:1:1 ratio (capture); (b) after adding 1.0 equiv of $\text{Zn}(\text{OTf})_2$, furnishing $[\text{Zn}(\text{I})]^{2+}$ and $[\text{Ag}(\text{II})]^+$ (release); (c) after addition of 1.0 equiv of hexacyclen; (d) after adding 1.0 equiv of $\text{Zn}(\text{OTf})_2$; (e) after addition of 1.0 equiv of hexacyclen.

Although silver(I) in $[\text{Ag}(\text{II})]^+$ is coordinated to the azacrown unit, we expected it to be active in catalysis and actually somewhat stabilized against decomposition. Indeed, when substrate **A** (100 mol %) was treated with $[\text{Ag}(\text{II})]^+$ (5 mol %) in $\text{CD}_2\text{Cl}_2:\text{CD}_3\text{CN} = 50:1$ at 40 °C for 2 h, isoquinoline-2-oxide **B**¹³ formed in $(45 \pm 2)\%$ (Scheme 3).

Scheme 3. Formation of Isoquinoline-2-oxide



Under identical conditions, 5 mol % of AgBF_4 furnished **B** in $(52 \pm 2)\%$. This reaction was completely shut down in the presence of **1** (5 mol %). Obviously, the silver(I) ions get scavenged inside nanoswitch **1** where they are catalytically inactive.

To probe the catalytic activity over several catch-release cycles (Figure 5), we started with 5 mol % of $[\text{Ag}(\text{II})]^+$ and

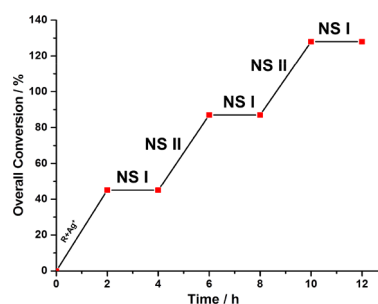


Figure 5. ON/OFF regulation of silver(I)-catalyzed formation of isoquinoline-2-oxide **B**. NS = NetState.

reactant **A** (100 mol %) yielding $(45 \pm 2)\%$ of **B** (after 2 h at 40 °C). After addition of nanoswitch **1** to return to NetState-I no further product is formed. Addition of 1.0 equiv of $\text{Zn}(\text{OTf})_2$ (5 μL of standard solution in acetonitrile) resulted in regeneration of NetState-II. The resultant mixture was heated for 2 h at 40 °C yielding $(43 \pm 2)\%$ of **B** (yield determined in 3 independent runs). Notably, this catalytic activity was almost the same as that of $[\text{Ag}(\text{II})]^+$ in absence of $[\text{Zn}(\text{I})]^{2+}$. To return to NetState I, 1 equiv of hexacyclen was added and the consumed amount of substrate was supplemented. Upon heating for 2 h under standard conditions no further product was detected by ^1H NMR. This implies that silver(I) was translocated back to nanoswitch **1** so that the silver ions are blocked for catalysis. In the third cycle still $(41 \pm 2)\%$ of product **B** was obtained in NetState II. Further catalytic cycles could not be performed due to poor solubility of the zwitterionic product.

Despite the small decrease of yield ($45\% \rightarrow 43\% \rightarrow 41\%$) over three release/capture cycles, possibly due a minor degradation of silver(I), a phenomenon equally seen in the fluorescence (Figure 2C), the catalytic activity remains elevated. In contrast, when the zinc(II)-triggered release of silver(I) from $[\text{Ag}(\text{I})]^+$ was run in absence of receptor **2**, the yields rapidly decayed: $(44 \pm 2)\%$ of **B** in the first cycle, then $(13 \pm 2)\%$ and finally $(6 \pm 2)\%$. Likewise, silver(I) alone is less suitable as reusable catalytic system. While AgBF_4 afforded $(52 \pm 2)\%$ of **B** in the first run, the second and third one with replenished reactant yielded only $(20 \pm 2)\%$ and $(11 \pm 2)\%$,

respectively. Clearly, the NetState I/II system provides superior catalytic activity in recycling schemes.

Moreover, there is a paramount advantage in using $[\text{Ag}(2)]^+$ as catalyst. Both the fluorescence intensity at $\lambda = 472$ nm and product conversion in the catalytic reaction are linearly correlated (Figure 6). Hence, the activity of the catalytic system can be followed or predicted by the emission intensity.

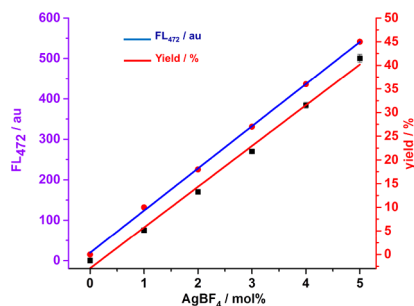
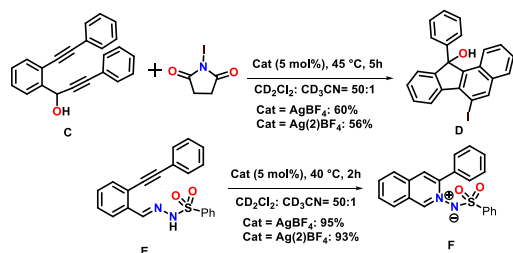


Figure 6. Fluorescence ($\lambda = 472$ nm) and yield of **B** depending on the amount of AgBF_4 in the presence of **2** (5 mol %).

The utility of the luminescent $[\text{Ag}(2)]^+$ catalyst goes far beyond the preparation of **B**, because it showed a catalytic activity basically as high as that of silver(I) also in other transformations^{14,15} (Scheme 4), so that it should work equally in other catch–release applications.

Scheme 4. Reactions in the Presence of Two Silver(I) Catalysts



In conclusion, the present multifunctional system in which nanoswitch **1** is networked to ligand **2** through chemical signaling¹⁶ designed for stepless regulation including status report of silver(I) catalytic activity by fluorescence is a supreme example for the practical utility of molecular communication.^{7,8} A pivotal factor of the system is the luminescent catalyst $[\text{Ag}(2)]^+$ whose activity is basically as high as that of neat silver(I).¹⁷ $[\text{Ag}(2)]^+$ is stable as solution over 7 days at ambient conditions (free Ag^+ decomposes within 1 d, see Figure S66), its robustness even at 10^{-8} M can be qualitatively judged via naked-eye testing of the emission color and an exact assessment of its catalytic activity is possible by ratiometric luminescence assay.

■ ASSOCIATED CONTENT

Supporting Information

The Supporting Information is available free of charge on the ACS Publications website at DOI: 10.1021/jacs.9b01182.

Synthetic procedures, characterization of substrates and metal complexes, NMR spectra, ESI-MS spectra, UV–vis studies, measurements of binding constants and

catalytic studies, and crystallographic data and experimental details of the structural refinement (PDF)

■ AUTHOR INFORMATION

Corresponding Author

*schmittel@uni-siegen.de

ORCID

Soumen De: 0000-0003-4674-9183

Michael Bolte: 0000-0001-5296-6251

Michael Schmittel: 0000-0001-8622-2883

Notes

The authors declare no competing financial interest.

■ ACKNOWLEDGMENTS

We are grateful to the Deutsche Forschungsgemeinschaft (Schm 647/19-2) and Universität Siegen for financial support. We thank STOE & Cie. (Darmstadt, Germany) for the opportunity to measure the data set. Dedicated to Prof. Dr. H.-D. Lutz (Siegen) on the occasion of his 85th birthday.

■ REFERENCES

- (1) *Applied Homogeneous Catalysis with Organometallic Compounds*, 3rd ed.; Cornils, B., Herrmann, W. A., Beller, M., Paciello, R., Eds.; Wiley-VCH: Weinheim, 2017.
- (2) (a) Tan, X.; Liu, Z.; Shen, H.; Zhang, P.; Zhang, Z.; Li, C. Silver-Catalyzed Decarboxylative Trifluoromethylation of Aliphatic Carboxylic Acids. *J. Am. Chem. Soc.* **2017**, *139*, 12430–12433. (b) Yang, S.; Rui, K.-H.; Tang, X.-Y.; Xu, Q.; Shi, M. Rhodium/Silver Synergistic Catalysis in Highly Enantioselective Cycloisomerization/Cross Coupling of Keto-Vinylidene-cyclopropanes with Terminal Alkynes. *J. Am. Chem. Soc.* **2017**, *139*, 5957–5964.
- (3) (a) Clarke, A. K.; Lynam, J. M.; Taylor, R. J. K.; Unsworth, W. P. Back-to-Front” Indole Synthesis Using Silver(I) Catalysis: Unexpected C-3 Pyrrole Activation Mode Supported by DFT. *ACS Catal.* **2018**, *8*, 6844–6850. (b) Tata, R. R.; Fu, C.; Kelley, S. P.; Harmata, M. Synthesis of 3-(Arylsulfonyl)-3-pyrrolines from Allenyl Sulfonamides by Silver Ion Catalysis. *Org. Lett.* **2018**, *20*, 5723–5726. (c) Zhu, Y.; He, W.; Wang, W.; Pitsch, C. E.; Wang, X.; Wang, X. Enantioselective Tandem Cyclization of Alkyne-Tethered Indoles Using Cooperative Silver(I)/Chiral Phosphoric Acid Catalysis. *Angew. Chem., Int. Ed.* **2017**, *56*, 12206–12209.
- (4) Lo, V. K.-Y.; Chan, A. O.-Y.; Che, C.-M. Gold and silver catalysis: From organic transformation to bioconjugation. *Org. Biomol. Chem.* **2015**, *13*, 6667–6680.
- (5) Gruttadauria, M.; Giacalone, F.; Noto, R. Release and catch” catalytic systems. *Green Chem.* **2013**, *15*, 2608–2618.
- (6) Sinha, I.; Mukherjee, P. S. Chemical Transformations in Confined Space of Coordination Architectures. *Inorg. Chem.* **2018**, *57*, 4205–4221.
- (7) Neamtu, M.; Nadejde, C.; Hodoroaba, V.-D.; Schneider, R. J.; Verestiuc, L.; Panne, U. Functionalized magnetic nanoparticles: Synthesis, characterization, catalytic application and assessment of toxicity. *Sci. Rep.* **2018**, *8*, 6278.
- (8) Remón, P.; Pischel, U. Chemical Communication between Molecules. *ChemPhysChem* **2017**, *18*, 1667–1677.
- (9) (a) Ray, D.; Foy, J. T.; Hughes, R. P.; Aprahamian, I. A switching cascade of hydrazone-based rotary switches through coordination-coupled proton relays. *Nat. Chem.* **2012**, *4*, 757–762. (b) Pramanik, S.; De, S.; Schmittel, M. Bidirectional Chemical Communication between Nanomechanical Switches. *Angew. Chem., Int. Ed.* **2014**, *53*, 4709–4713. (c) Pramanik, S.; De, S.; Schmittel, M. A Trio of Nanoswitches in Redox-Potential Controlled Communication. *Chem. Commun.* **2014**, *50*, 13254–13257. (d) Ren, Y.; You, L. Dynamic Signaling Cascades: Reversible Covalent Reaction-Coupled Molecular Switches. *J. Am. Chem. Soc.* **2015**, *137*, 14220–14228.

- (10) Mittal, N.; Pramanik, S.; Paul, I.; De, S.; Schmittel, M. Networking Nanoswitches for ON/OFF Control of Catalysis. *J. Am. Chem. Soc.* **2017**, *139*, 4270–4273.
- (11) Goswami, A.; Pramanik, S.; Schmittel, M. Catalytically active nanorotor reversibly self-assembled by chemical signaling within an eight-component network. *Chem. Commun.* **2018**, *54*, 3955–3958.
- (12) (a) He, Z.; Jiang, W.; Schalley, C. A. Integrative self-sorting: a versatile strategy for the construction of complex supramolecular architecture. *Chem. Soc. Rev.* **2015**, *44*, 779–789. (b) Lal Saha, M.; Schmittel, M. Degree of molecular self-sorting in multicomponent systems. *Org. Biomol. Chem.* **2012**, *10*, 4651–4684.
- (13) Zhao, X.; Fan, W.; Miao, Z.; Chen, R. Efficient Synthesis of Isoquinoline Derivatives via AgOTf/Cu(OTf)₂-Cocatalyzed Cyclization of 2-Alkynyl Benzaldoxime. *Synth. Commun.* **2013**, *43*, 1714–1720.
- (14) Chen, Z.; Zeng, M.; Yuan, J.; Yang, Q.; Peng, Y. Novel Silver Tetrafluoroborate Catalyzed Electrophilic Cascade Cyclization Reaction: A Facile Approach to the Synthesis of Halo-Substituted Benzo[a]fluorens. *Org. Lett.* **2012**, *14*, 3588–3591.
- (15) Cheng, X.; Cao, X.; Xuan, J.; Xiao, W.-J. Silver(I)- and Base-Mediated [3 + 3]-Cycloaddition of C₃N-Cyclic Azomethine Imines with Aza-oxyallyl Cations. *Org. Lett.* **2018**, *20*, 52–55.
- (16) Castilla, A. M.; Ronson, T. K.; Nitschke, J. R. Sequence-Dependent Guest Release Triggered by Orthogonal Chemical Signals. *J. Am. Chem. Soc.* **2016**, *138*, 2342–2351.
- (17) Wang, W.; Cui, L.; Sun, P.; Shi, L.; Yue, C.; Li, F. Reusable N-Heterocyclic Carbene Complex Catalysts and Beyond: A Perspective on Recycling Strategies. *Chem. Rev.* **2018**, *118*, 9843–9929.